

Learning Displacement-Aware WiFi Representations for Weakly Supervised Relative Localization

Tzu-Ti Wei, Po-Cheng Chen, Yu-Chee Tseng, Jen-Jee Chen
 College of AI, National Yang Ming Chiao Tung University, Taiwan
 { a2699560.ai09, havefree456.c, yctsens, jenje }@nycu.edu.tw

Abstract—WiFi fingerprint-based indoor localization has been widely studied, but most existing approaches focus on absolute positioning and rely on dense coordinate annotations, which are costly to obtain at scale. In this paper, we study a fundamentally different problem: *relative localization*, where the goal is to directly estimate the displacement between two WiFi fingerprint traces without predicting their absolute positions. To reduce annotation overhead, we adopt weak supervision in the form of stepwise motion vectors obtained from inertial sensing. We propose *Intersection Pathway (IP)*, a cross-modal learning framework that aligns *fingerprint traces (f-traces)* and *displacement traces (d-traces)* in a shared latent space. The key idea is to enforce an *additive structure* in the latent space, such that latent addition and subtraction correspond to physical motion composition, enabling direct relative-displacement inference. Experiments on a synthesized dataset derived from real measurements demonstrate that the proposed method learns *displacement-aware* WiFi representations and achieves accurate relative localization across varying displacement ranges. Furthermore, the learned model can be extended to few-shot absolute localization with sparse anchors.

Index Terms—indoor localization, WiFi fingerprint, weak supervision, multimodal learning, relative localization

I. INTRODUCTION

Indoor positioning is a key enabler of location-based services [1], [2]. Existing approaches span inertial-, RF- and vision-based techniques [3]–[6]. Among them, WiFi fingerprinting is particularly attractive due to the ubiquitous deployment of WiFi infrastructures [7]. Conventional WiFi localization methods map RSSI/CSI fingerprints, or short fingerprint sequences, to absolute coordinates [8]–[10]. However, such approaches rely on *strong* supervision—dense location annotations—which are costly and difficult to obtain at scale.

In this paper, we address a fundamentally different problem: *relative localization*. Given two WiFi fingerprint traces corresponding to objects A and B , our goal is to directly estimate the displacement Δ_{AB} from A to B , without explicitly predicting their absolute positions. This formulation is particularly relevant in scenarios such as robot following, warehouse coordination, and human-object interaction, where relative spatial relationships are more actionable than global coordinates. This raises a key question: *Can relative displacement be learned directly from weak supervision, without dense coordinate labels?* Fig. 1 illustrates the conceptual difference between the proposed setting and conventional absolute localization.

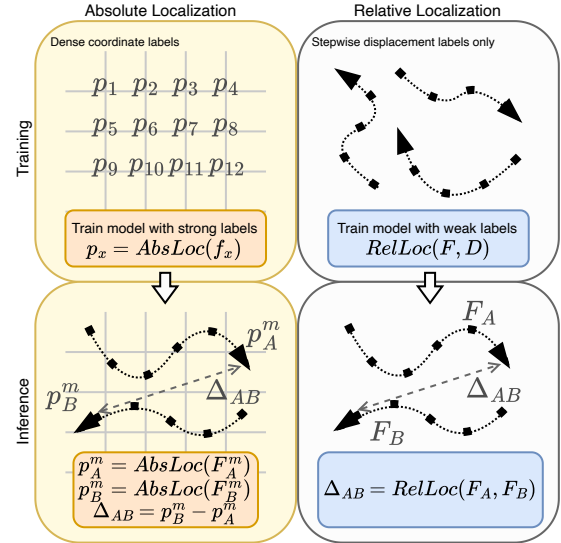


Fig. 1. A conceptual comparison between conventional absolute localization and the proposed relative localization. Here, F denotes a WiFi fingerprint trace and D denotes a displacement trace used as weak supervision.

Prior work on WiFi-based indoor localization has primarily focused on improving absolute positioning accuracy. Deep learning approaches have been widely adopted to mitigate fingerprint ambiguity and noise [11]–[15], while crowdsourcing techniques aim to construct or refine large-scale fingerprint maps [16]–[19]. Systems such as BlindNavi [20] and UbiFin [21] demonstrate the feasibility of real-world deployment.

However, these approaches consistently rely on absolute localization with dense coordinate annotations, and do not address the problem of learning relative displacement under weak supervision. Moreover, unlike systems based on UWB, BLE tags, or WiFi FTM, our setting does not assume specialized hardware or explicit ranging capabilities, making it more broadly applicable in commodity WiFi environments.

To reduce labeling cost, we rely solely on *weak* supervision in the form of stepwise motion vectors between adjacent samples, which can be obtained with low overhead from inertial sensors on robots or simple IoT devices. Our goal is to eliminate the need for dense coordinate annotations.

To this end, we propose *Intersection Pathway (IP)*, a cross-modal learning framework that makes WiFi fingerprints *computable in the displacement domain*. Specifically, IP maps fingerprint traces and displacement traces into a shared latent

space, where local motion relations regularize fingerprint representations. By enforcing that latent addition and subtraction correspond to physical motion composition, the model enables direct *displacement-aware inference* from fingerprint traces.

The main contributions of this work are as follows:

- We formulate WiFi-based *relative localization* as a weakly supervised problem, enabling direct displacement estimation without dense coordinate labels.
- We propose *Intersection Pathway*, a cross-modal framework that aligns fingerprint and displacement traces in a shared latent space, where latent addition and subtraction correspond to physical motion. This effectively induces a displacement-aware latent space in which WiFi fingerprints inherit the additive structure of physical motion.
- We show that the learned representation supports both relative localization and a lightweight extension to few-shot absolute localization with sparse anchors.

II. PROBLEM FORMULATION

We consider a 2D indoor field with n WiFi access points. A moving device collects two synchronized traces along a trajectory of length m : an *f-trace* $F = (f_1, \dots, f_m)$ and a *d-trace* $D = (d_1, \dots, d_m)$. Each fingerprint $f_i = (s_1, \dots, s_n)$ records RSSI values from nearby APs, while each displacement vector d_i represents the stepwise motion between two adjacent sampling points. More specifically, if the trajectory positions are (p_1, p_2, \dots, p_m) , then $d_i \approx \overrightarrow{p_{i-1}p_i}$ for $i = 2, \dots, m$, and we set $d_1 = \vec{0}$ as the initial placeholder. We regard D as a *weak label* of F because it contains only relative motions rather than absolute coordinates.

Given a crowdsourced dataset \mathcal{D} of paired traces (F, D) , our goal is to learn a model that takes two f-traces F_A and F_B as input and predicts the displacement from the endpoint of F_A to the endpoint of F_B . Formally, if the endpoints of the two traces are p_A^m and p_B^m , respectively, then the target is

$$\Delta_{AB} = \overrightarrow{p_A^m p_B^m} = p_B^m - p_A^m. \quad (1)$$

That is, we aim to learn a function

$$\text{RelLoc}(F_A, F_B) \approx \Delta_{AB}. \quad (2)$$

As illustrated conceptually in Fig. 1, this differs from conventional absolute localization, which first estimates two global coordinates and then subtracts them. Our formulation directly targets the relative displacement and is therefore better aligned with applications in which one mobile entity needs to locate another.

The key challenge is to make WiFi fingerprints *computable* in the displacement domain. Fingerprints are ambiguous and noisy, whereas physical displacements are additive. The corresponding method design is presented in the next section.

III. METHOD

Figs. 2 and 3 illustrate the proposed framework. At a high level, our design consists of two autoencoders that share one latent space: one processes *f-traces* and the other processes *d-traces*. On top of these two branches, we construct direct

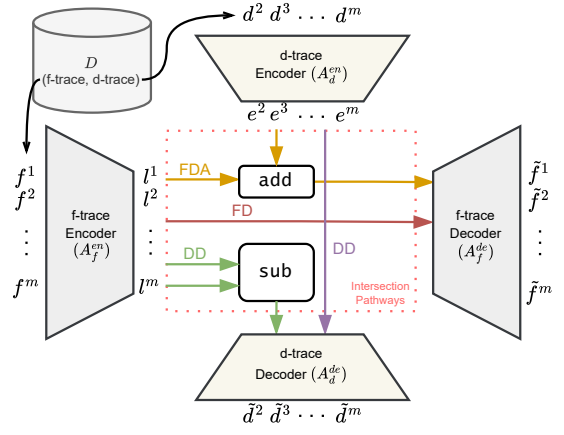


Fig. 2. Training architecture of the proposed Intersection Pathway (IP), which takes paired *f-trace* and *d-trace* as input.

pathways for reconstruction and cross-modal pathways for interaction between fingerprints and motions. This design allows local motion relations to regularize fingerprint relations, so that latent-space addition and subtraction become meaningful for relative-position inference. The autoencoders are therefore not introduced merely for exact input reconstruction; rather, they are used to learn a shared latent space in which fingerprint context can be regularized and displacement composition can be preserved. During training, the model takes a paired input (F, D) from \mathcal{D} . During inference, it takes two *f-traces* F_A and F_B , and directly predicts the endpoint displacement from A to B by decoding the difference between their endpoint latent codes through the *d-trace* branch.

F-trace autoencoder: An *f-trace* is a short sequence of WiFi fingerprints, so similar fingerprints may appear at different positions and a single sample may fluctuate over time. To handle this ambiguity, we encode each *f-trace* with a transformer-based autoencoder. The *f-trace* encoder maps $F = (f_1, \dots, f_m)$ to latent codes

$$A_f^{en}(F) = (l_1, \dots, l_m), \quad (3)$$

where each code captures both the current fingerprint and its sequential context. The corresponding decoder reconstructs the input trace as

$$A_f^{de}(l_1, \dots, l_m) = (\tilde{f}_1, \dots, \tilde{f}_m). \quad (4)$$

This sequential modeling is important because the meaning of one fingerprint becomes clearer when its upstream and downstream context is also considered. The reconstruction branch is used to stabilize these context-aware embeddings under noisy RSSI observations, rather than to assume that unseen traces must be reconstructed perfectly.

D-trace autoencoder: Each displacement vector d_i is mapped to a latent code e_i by a linear autoencoder. The *d-trace* encoder maps $D = (d_1, \dots, d_m)$ to

$$A_d^{en}(D) = (e_1, \dots, e_m), \quad (5)$$

and the decoder maps the latent displacement codes back to reconstructed displacements,

$$A_d^{de}(e_1, \dots, e_m) = (\tilde{d}_1, \dots, \tilde{d}_m). \quad (6)$$

We deliberately keep this branch linear so that physical additivity is preserved in the latent space. The latent dimensionality of e_i is matched to that of l_i , enabling the two modalities to interact directly. Here the autoencoder serves to place displacement vectors into the shared latent space while preserving their additive structure, rather than merely reconstructing them. This linearity is essential because our inference relies on latent-space addition and subtraction to compose or compare displacements.

Intersection Pathway: To align the two modalities, we use four training pathways based on the above encoders and decoders. The four pathways are defined as follows.

Fingerprint-Direct (FD): this pathway reconstructs the input f -trace and is trained with

$$L_{FD} = \sum_{i=1}^m |f_i - \tilde{f}_i|. \quad (7)$$

Displacement-Direct (DD): this pathway reconstructs the input d -trace and is trained with

$$L_{DD} = \sum_{i=2}^m |d_i - \tilde{d}_i|. \quad (8)$$

Fingerprint-Displacement-Add (FDA): this pathway injects local motion into the fingerprint latent space. Here, l_{i-1} is the latent code of fingerprint f_{i-1} , e_i is the latent code of displacement d_i , \hat{l}_i is the estimated latent code of the next fingerprint, and \hat{f}_i is its decoded reconstruction. Intuitively, starting from the latent code of the previous fingerprint, we add the latent displacement corresponding to the motion from p_{i-1} to p_i and expect the result to match the latent code of the next fingerprint. Formally,

$$\hat{l}_i = \begin{cases} l_i, & i = 1, \\ l_{i-1} + e_i, & i = 2, \dots, m, \end{cases} \quad (9)$$

and the resulting latent sequence is decoded as

$$(\hat{f}_1, \dots, \hat{f}_m) = A_f^{de}(\hat{l}_1, \dots, \hat{l}_m). \quad (10)$$

This pathway encourages the model to make latent addition correspond to physical motion transitions in the fingerprint domain. The loss is

$$L_{FDA} = \sum_{i=1}^m |f_i - \hat{f}_i|. \quad (11)$$

Fingerprint-Fingerprint-Subtract (FFS): this pathway performs the reverse interaction. Here, $l_i - l_{i-1}$ represents the latent difference between two adjacent fingerprints, \hat{e}_i is the estimated latent code of displacement d_i , and \hat{d}_i is the decoded

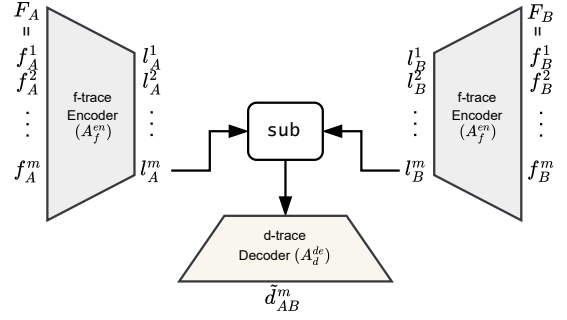


Fig. 3. Inference architecture of the proposed Intersection Pathway (IP), which takes two f -traces (F_A, F_B) and predicts their relative displacement \tilde{d}_{AB}^m .

displacement in the physical space. It estimates local displacement from two adjacent fingerprint latents and requires the decoded result to match the stepwise motion label. Formally,

$$\hat{e}_i = \begin{cases} \vec{0}, & i = 1, \\ l_i - l_{i-1}, & i = 2, \dots, m, \end{cases} \quad (12)$$

and the estimated displacement is decoded as

$$(\hat{d}_1, \dots, \hat{d}_m) = A_d^{de}(\hat{e}_1, \dots, \hat{e}_m). \quad (13)$$

This pathway encourages latent subtraction between adjacent fingerprints to correspond to physical displacement. The loss is

$$L_{FFS} = \sum_{i=2}^m |d_i - \hat{d}_i|. \quad (14)$$

Training proceeds in three stages:

$$\begin{aligned} L_{phase1} &= L_{FD}, \\ L_{phase2} &= L_{FD} + L_{FDA}, \\ L_{phase3} &= L_{FD} + L_{DD} + L_{FFS}. \end{aligned} \quad (15)$$

In the first stage, we use only L_{FD} so that the model can learn robust latent representations of f -traces from sequential WiFi fingerprints, which is particularly important for resolving fingerprint ambiguity. In the second stage, we introduce L_{FDA} to inject local motion information into the fingerprint latent space, so that latent addition starts to reflect transitions between adjacent fingerprints. In the third stage, we further optimize L_{DD} and L_{FFS} so that physical displacements can be stably mapped to and from the latent space, and latent differences between adjacent fingerprints become aligned with displacement vectors.

At inference time as shown in Fig. 3, two f -traces F_A and F_B are encoded into (l_A^1, \dots, l_A^m) and (l_B^1, \dots, l_B^m) . The predicted relative displacement is

$$\hat{\Delta}_{AB} = \tilde{d}_{AB}^m = A_d^{de}(l_B^m - l_A^m), \quad (16)$$

where A_d^{de} is the d -trace decoder. Intuitively, the model translates endpoint differences in the fingerprint latent space into displacement vectors in the physical space. The linear d -trace branch is critical here because it preserves the additivity

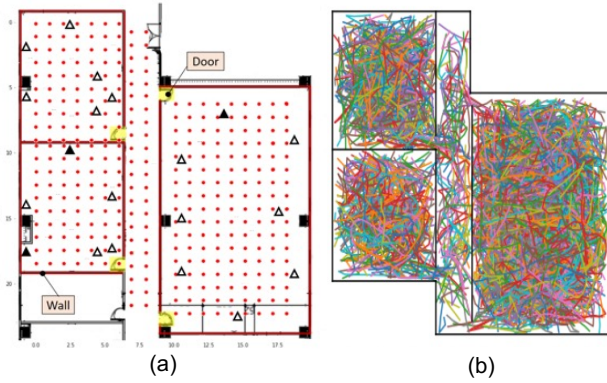


Fig. 4. Dataset collection: (a) locations with manually collected WiFi fingerprints and AP placements, where solid and hollow triangles denote 2.4 GHz and dual-band (2.4+5 GHz) APs, respectively; and (b) synthesized trajectories in the target field.

needed to generalize from short stepwise supervision to longer relative displacements.

IV. EXPERIMENTS

A. Dataset

Our experimental field is a concrete indoor space of roughly 20×25 meters with several rooms and a corridor, as illustrated in Fig. 4(a). It contains 20 WiFi APs and 337 labeled locations, with around 50 RSSI fingerprints collected at each location. Since a large real paired dataset of f -traces and d -traces is difficult to obtain, we build a near-real dataset for training and evaluation.

We collect (i) dense WiFi fingerprints in the experimental field and (ii) human walking trajectories in other fields, and synthesize a large dataset as follows.

- 1) We repeatedly selected a trajectory from (ii) and cropped a length- m sub-trajectory. These sub-trajectories formed a dataset \mathcal{D}_{traj} .
- 2) We repeatedly sampled a trajectory $t \in \mathcal{D}_{traj}$ and a point p in the experimental field. We shifted the starting point of t to p and randomly rotated it. If the trajectory does not hit any wall, we include it in a synthesized dataset \mathcal{D}_{sy} .
- 3) From each trajectory in \mathcal{D}_{sy} , we derived a d -trace and a f -trace. For each point in the trajectory, if it fell in one of the labeled 337 locations, we sampled a WiFi fingerprint for it; otherwise, we synthesized one by Gaussian process regression (GPR) [22].

Fig. 4(b) shows that trajectories in \mathcal{D}_{sy} cover the target field well. The dataset is near-real rather than fully real-world: trajectory geometry comes from real motion traces, while RSSI fingerprints are queried from the target-field map after each transformed trajectory is placed in that field, with GPR used only for unlabeled points. To mimic deployment noise, we perturb both modalities. For any WiFi RSSI f_u , we inject noise by

$$\hat{f}_u = f_u \times (1 + N(0, \sigma_f)), \quad (17)$$

where σ_f is a predefined standard deviation. For any displacement vector (d_x, d_y) , we convert it into a distance r and an angle θ , and perturb them by

$$\begin{aligned} \hat{d}_r &= r \times (1 + N(0, \sigma_r)), \\ \hat{d}_\theta &= \theta + N(0, \sigma_\theta). \end{aligned} \quad (18)$$

We then convert $(\hat{d}_r, \hat{d}_\theta)$ back into a displacement vector (\hat{d}_x, \hat{d}_y) . Unless otherwise stated, we use 40K synthesized traces with $m = 9$, set $(\sigma_f, \sigma_r, \sigma_\theta) = (0.05, 0.2, 0.15)$, and split the data into training and testing sets at a ratio of 8:2.

B. Evaluation Metrics

The relative localization problem has no widely adopted standard benchmark, so we use two complementary metrics.

Displacement Error (DE): This metric measures the mean Euclidean error between the predicted relative displacement and the target relative displacement. Let

$$\hat{\Delta}_{AB} = A_d^{de} (l_B^m - l_A^m) \quad (19)$$

be the predicted displacement from the endpoint of F_A to that of F_B , and let Δ_{AB} denote the target displacement defined in Sec. II. We then define

$$DE = \frac{1}{N} \sum \left| \hat{\Delta}_{AB} - \Delta_{AB} \right|, \quad (20)$$

where N is the number of sampled pairs. Since our data provide only weak displacement supervision and displacement difficulty grows with distance, we further report

$$DE(k) = \frac{1}{N'} \sum_{|\Delta_{AB}| \leq k} \left| \hat{\Delta}_{AB} - \Delta_{AB} \right|, \quad (21)$$

where N' is the number of sampled pairs whose target displacement length is at most k meters. In particular, we report $DE(5)$, $DE(10)$, and $DE(all)$.

Latent Code-Distance Ratio (LCDR): This metric evaluates whether latent-space distances scale consistently with physical displacements. Since sampled pairs may still have slightly different displacement lengths, we first normalize each latent distance by its target displacement length. Consider two sampled pairs (F_A, F_B) and (F_C, F_D) such that $|\Delta_{AB}| \approx |\Delta_{CD}|$. We define

$$r_{AB} = \frac{|l_B^m - l_A^m|}{|\Delta_{AB}|}, \quad r_{CD} = \frac{|l_D^m - l_C^m|}{|\Delta_{CD}|}. \quad (22)$$

If the learned latent space preserves displacement structure well, then pairs with similar physical displacements should also have similar normalized latent distances. We therefore define

$$LCDR_{A,B,C,D} = \frac{\min\{r_{AB}, r_{CD}\}}{\max\{r_{AB}, r_{CD}\}}. \quad (23)$$

A value closer to 1 indicates better scaling consistency between latent-space distances and physical displacements. Over all sampled pairs, we compute

$$LCDR = \frac{1}{N} \sum LCDR_{A,B,C,D}, \quad (24)$$

TABLE I
RELATIVE LOCALIZATION PERFORMANCE AND KEY ABLATIONS.

Method	$DE(5)$	$DE(10)$	$DE(all)$
LSTM backbone	0.300	0.885	1.818
DNN backbone	0.575	1.034	1.961
w/o A_d^{en}	0.469	0.941	1.842
w/o A_d^{en}, A_f^{de}	0.710	1.544	3.324
nonlinear A_d	1.505	2.707	4.672
Ours	0.329	0.719	1.751

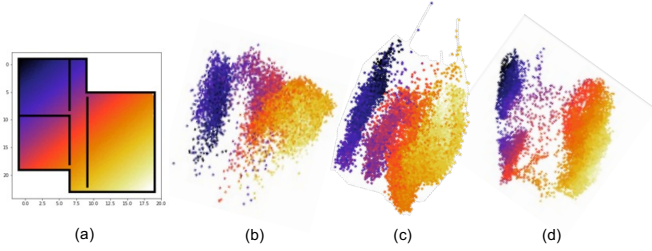


Fig. 5. Coherence of latent codes with the physical map: (a) the physical map with color assignment by locations, and (b)–(d) PCA plots of endpoint latent codes after progressively longer stage-wise training.

and similarly define

$$LCDR(k) = \frac{1}{N'} \sum_{|\Delta_{AB}| \leq k} LCDR_{A,B,C,D}. \quad (25)$$

C. Performance Evaluation

Direct comparison with prior WiFi localization methods is not straightforward because most of them target absolute localization with strong labels [8]–[10], [12]–[15]. In contrast, our task infers relative displacement from paired f -traces under weak displacement supervision. We therefore focus on unified performance evaluation and controlled ablations, with few-shot absolute localization as a complementary reference.

Table I shows that our method achieves the best overall performance on $DE(10)$ and $DE(all)$, indicating that the shared latent space learned by IP captures longer-range spatial relations better than the alternatives. For the f -trace backbone, the DNN variant performs poorly, while the LSTM backbone achieves the best $DE(5)$ but degrades more noticeably as the displacement range increases, suggesting that feed-forward or purely recurrent modeling is still limited for displacement composition over longer ranges.

The ablation variants further validate the proposed design. In “w/o A_d^{en} ”, the d -trace encoder is removed, so displacement traces are no longer encoded into the shared latent space and the DD and FDA pathways are disabled accordingly. In “w/o A_d^{en}, A_f^{de} ”, we further remove the f -trace decoder, which also disables the FD pathway. The performance drops of these two variants show that both the cross-modal interaction and the reconstruction pathway contribute to stable relative-localization learning. Replacing the linear d -trace branch by a nonlinear one (“nonlinear A_d ”) leads to the largest degra-

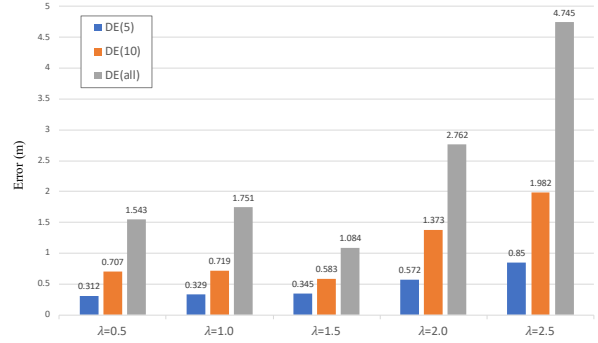


Fig. 6. Impact of noise strength by varying λ .

TABLE II
IMPACT OF TRACE LENGTH AND DATASET SIZE.

	$DE(5)$	$DE(10)$	$DE(all)$	$LCDR(5)$	$LCDR(10)$	$LCDR(all)$
$m = 5$	0.574	1.138	2.272	0.686	0.595	0.542
$m = 7$	0.322	0.813	2.077	0.715	0.594	0.542
$m = 9$	<u>0.329</u>	<u>0.719</u>	<u>1.751</u>	0.744	<u>0.641</u>	<u>0.592</u>
$m = 11$	0.446	0.559	1.037	0.690	0.642	0.638
$ \mathcal{D} = 4K$	0.910	2.403	5.472	0.636	0.523	0.446
$ \mathcal{D} = 12K$	<u>0.696</u>	<u>1.272</u>	<u>2.267</u>	0.618	<u>0.554</u>	<u>0.535</u>
$ \mathcal{D} = 40K$	0.329	0.719	1.751	0.744	0.641	0.592

ation, confirming that linearity is important for preserving displacement composition in the latent space, which is exactly the property required by latent addition and subtraction during inference.

D. Training Dynamics and Sensitivity Analyses

We further examine how the latent space evolves during training. Fig. 5 shows the latent codes of the endpoints of 40K f -traces after PCA projection. In the early stage, the model mainly captures local signal-spatial correlations. As stage-2 and stage-3 training continue, the latent codes become increasingly coherent with the physical layout, indicating that the proposed staged training gradually aligns fingerprint relations with displacement structure.

To evaluate robustness, we vary the noise strength for both f -traces and d -traces by scaling $(\sigma_f, \sigma_r, \sigma_\theta)$ with a factor λ . Fig. 6 shows that the model remains stable when $\lambda \leq 2.0$, but degrades sharply at $\lambda = 2.5$. This suggests that the proposed framework can tolerate moderate sensing noise, while excessive perturbation weakens the learned fingerprint-displacement alignment.

Table II further studies the impact of trace length and dataset size. Longer traces generally improve geometric consistency and long-range localization performance, although very short-range accuracy does not always monotonically improve. Increasing the dataset size consistently improves both DE and LCDR, confirming that the model benefits from broader spatial coverage and richer local transitions.

E. Few-shot Absolute Localization Extension

Although our model is trained for relative localization, it can be extended to absolute localization by using a sparse set of anchor traces with known endpoints. Given a query trace

TABLE III
FEW-SHOT ABSOLUTE LOCALIZATION UNDER VARYING NOISE STRENGTHS (λ) AND TRACE LENGTHS (m).

	no noise	$\lambda = 0.5$	$\lambda = 1.0$	$\lambda = 1.5$	$\lambda = 2.0$	$\lambda = 2.5$	$m = 5$	$m = 7$	$m = 9$	$m = 11$
LSTM-loc	0.129	0.144	0.146	0.170	0.181	0.196	0.171	0.159	0.146	0.138
BERT-loc	0.039	0.060	0.064	0.097	0.119	0.135	0.070	0.070	0.064	0.062
ours	0.140	0.312	0.329	0.345	0.572	0.850	0.574	0.322	0.329	0.446

F_B , we compute its relative displacement to each anchor trace F_A , recover the endpoint of F_B from the anchor endpoint plus the predicted displacement, and use the anchor producing the shortest predicted displacement as the final reference.

Table III summarizes the few-shot absolute-localization performance under varying noise strengths and trace lengths. LSTM-loc and BERT-loc are fully supervised baselines trained with strong labels for all traces, whereas our method uses weak labels for training and only sparse strong labels at inference time.

In the left half of Table III, the fully supervised baselines remain relatively stable as noise increases, whereas our method becomes more sensitive to stronger perturbation. In the right half, our method performs best at medium trace lengths, suggesting that very short traces provide insufficient context while overly long traces may accumulate more variation. Although our few-shot extension does not outperform fully supervised baselines, it achieves sub-meter accuracy while requiring far fewer strong labels.

V. CONCLUSION

We presented a weakly supervised framework for WiFi-based relative localization. Instead of predicting two absolute coordinates with dense strong labels, the proposed method directly estimates the displacement between two objects from their fingerprint traces. The core idea is Intersection Pathway, which aligns transformer-based WiFi embeddings and linear displacement embeddings in a shared latent space and makes latent addition/subtraction correspond to physical motion. Experiments show that this design yields strong relative-localization performance and that its key components, especially explicit cross-modal interaction and the linear d -trace branch, are both important. We further showed that the learned model can be extended to few-shot absolute localization with sparse anchors. Future work may explore crowdsourced data under our framework.

REFERENCES

- [1] F. Liu, J. Liu, Y. Yin, W. Wang, D. Hu, P. Chen, and Q. Niu, "Survey on wifi-based indoor positioning techniques," *IET communications*, vol. 14, no. 9, pp. 1372–1383, 2020.
- [2] S. Pasricha, "Overview of indoor navigation techniques," *Position, Navigation, and Timing Technologies in the 21st Century: Integrated Satellite Navigation, Sensor Systems, and Civil Applications*, vol. 2, pp. 1141–1170, 2020.
- [3] H. Liu, H. Darabi, P. Banerjee, and J. Liu, "Survey of wireless indoor positioning techniques and systems," *IEEE Transactions on Systems, Man, and Cybernetics, Part C*, vol. 37, no. 6, pp. 1067–1080, 2007.
- [4] H. Zhou, J. Yang, S. Deng, and W. Zhang, "Vtil: A multi-layer indoor location algorithm for rssi images based on vision transformer," *Engineering Research Express*, vol. 6, no. 1, p. 015069, 2024.
- [5] R. Harle, "A survey of indoor inertial positioning systems for pedestrians," *IEEE Communications Surveys & Tutorials*, vol. 15, no. 3, pp. 1281–1293, 2013.
- [6] B. Großwindhager, M. Stocker, M. Rath, C. A. Boano, and K. Römer, "Snaploc: An ultra-fast uwb-based indoor localization system for an unlimited number of tags," in *Int'l Conf. on Information Processing in Sensor Networks*, 2019, pp. 61–72.
- [7] S. Shang and L. Wang, "Overview of wifi fingerprinting-based indoor positioning," *IET Communications*, vol. 16, no. 7, pp. 725–733, 2022.
- [8] C. Du, B. Peng, Z. Zhang, W. Xue, and M. Guan, "Kf-knn: Low-cost and high-accurate fm-based indoor localization model via fingerprint technology," *IEEE Access*, vol. 8, pp. 197 523–197 531, 2020.
- [9] S.-P. Kuo, B.-J. Wu, W.-C. Peng, and Y.-C. Tseng, "Cluster-enhanced techniques for pattern-matching localization systems," in *IEEE Int. Conf. on Mobile Adhoc and Sensor Systems*, 2007.
- [10] S.-P. Kuo and Y.-C. Tseng, "A scrambling method for fingerprint positioning based on temporal diversity and spatial dependency," *IEEE Transactions on Knowledge and Data Engineering*, vol. 20, no. 5, pp. 678–684, 2008.
- [11] F. Alhomayani and M. H. Mahoor, "Deep learning methods for fingerprint-based indoor positioning: A review," *Journal of Location Based Services*, vol. 14, no. 3, pp. 129–200, 2020.
- [12] Y.-T. Liu, J.-J. Chen, Y.-C. Tseng, and F. Y. Li, "An auto-encoder multitask lstm model for boundary localization," *IEEE Sensors Journal*, vol. 22, no. 11, pp. 10 940–10 953, 2022.
- [13] L. Wang, S. Shang, and Z. Wu, "Research on indoor 3d positioning algorithm based on wifi fingerprint," *Sensors*, vol. 23, no. 1, p. 153, 2022.
- [14] Z. Ma and K. Shi, "Few-shot learning for wifi fingerprinting indoor positioning," *Sensors*, vol. 23, no. 20, p. 8458, 2023.
- [15] Y. Dong, T. Arslan, and Y. Yang, "An encoded lstm network model for wifi-based indoor positioning," in *IEEE Int'l Conf. on Indoor Positioning and Indoor Navigation*, 2022, pp. 1–6.
- [16] B. Lashkari, J. Rezazadeh, R. Farahbakhsh, and K. Sandrasegaran, "Crowdsourcing and sensing for indoor localization in iot: A review," *IEEE Sensors Journal*, vol. 19, no. 7, pp. 2408–2434, 2018.
- [17] C. Wu, Z. Yang, and C. Xiao, "Automatic radio map adaptation for indoor localization using smartphones," *IEEE Transactions on Mobile Computing*, vol. 17, no. 3, pp. 517–528, 2017.
- [18] Y. Zhao, Z. Zhang, T. Feng, W.-C. Wong, and H. K. Garg, "Graphips: Calibration-free and map-free indoor positioning using smartphone crowdsourced data," *IEEE Internet of Things Journal*, vol. 8, no. 1, pp. 393–406, 2020.
- [19] C. Luo, H. Hong, and M. C. Chan, "Piloc: A self-calibrating participatory indoor localization system," in *Int'l Symp. on Information Processing in Sensor Networks*, 2014, pp. 143–153.
- [20] H.-E. Chen, Y.-Y. Lin, C.-H. Chen, and I.-F. Wang, "Blindnavi: A navigation app for the visually impaired smartphone user," in *ACM Conf. on Human Factors in Computing Systems*, 2015, pp. 19–24.
- [21] J. Tan, H. Wu, K.-H. Chow, and S.-H. G. Chan, "Implicit multimodal crowdsourcing for joint rf and geomagnetic fingerprinting," *IEEE Transactions on Mobile Computing*, vol. 22, no. 2, pp. 935–950, 2023.
- [22] C. Williams and C. Rasmussen, "Gaussian processes for regression," *Advances in neural information processing systems*, vol. 8, 1995.